Feature Extraction from Segmented MRI Brain Tissues for Schizophrenia detection

D.Selvaraj
Department of Electronics and Communication Engineering
Sathyabama University
Chennai, India
mails2selvaraj@yahoo.com

R.Dhanasekaran
Department of Electrical and Electronics Engineering
Syed Ammal Engineering College
Ramanathapuram, India
rdhanashekar@yahoo.com

***Abstract*— Automated MRI (Magnetic Resonance Imaging) brain tumour segmentation is a difficult task due to the variance and complexity of tumours. In this paper, we explored a new method for extracting feature from the MRI brain image based on statistical structure analysis. At first, the input MRI brain image is segmented into normal tissues (white matter and gray matter), pathological tissues (tumour) and fluid (Cerebrospinal fluid). Later, these segmented tissue images are split into a limited number of small blocks of size 4x4 and the feature values are calculated for each block which quantify the intensity, symmetry and texture properties of different tissues. The extracted features can be used as an input to a classifier to detect the schizophrenia disease.**

***Index Terms*—Feature Extraction, Schizophrenia, Alzheimer.**

I. INTRODUCTION

Today, one of the major causes for the increase in fatality among children and adults is brain tumor. Most research in developed countries has exposed that the death rate of people affected by brain tumor has increased over the past three decades [1]. Magnetic resonance imaging (MRI) is an important diagnostic imaging technique for the early detection of abnormal changes in tissues and organs. It possesses good contrast resolution for different tissues and has advantages over computerized tomography (CT) for brain studies due to its superior contrast properties. Therefore, the majority of research in medical image segmentation pertains to its use for MR images, especially in brain imaging [2], [3].

The primary goal of brain image segmentation is to partition a given brain image in to nonintersecting regions representing true anatomical structures such as grey matter, white matter, and more. Due to the characteristics of MR images, development of automated segmentation algorithms is challenging. Because of inherent noise, partial volume effect and wide range of imaging parameters, which affect the tissue intensities, there is a significant inter-patient variation of signal intensities for the same tissues [4].There are several approaches to Brain MR image segmentation: discriminant analysis [5], neural networks [7], [8], clustering [6], brain atlases [9], knowledge-based techniques [10], shape-based models [11], [12], morphological operators [13], multivariate principal component analysis [14], pixel based models Expectation Maximization Algorithm [15], Multi-resolution edge detection [7] and statistical pattern recognition [16], to name a few.

Supervised segmentation methods have exhibited problems with reproducibility, due to significant intra and inter-observer variance introduced over multiple trials of training. Further they consume more time and needs domain expertise. So, supervised methods are unsuitable for clinical use. These limitations suggest the need for a fully automatic method for segmentation and classification. In unsupervised methods instead of feeding the input as raw image, features of the image are calculated and later it can be fed as input to the classifier so that the time consumption and storage space can be reduced.

The success of unsupervised segmentation and classification methods depend upon the effective features. Intensity based features are most widely used. But due to the complexity of the brain tissues, intensity based features alone cannot achieve acceptable result so, texture features are calculated along with intensity features. Co-occurrence matrix and wavelet based texture features are used to achieve promising results. In this paper, we have utilized the brain tissues segmented using the segmentation technique that we have proposed in our previous research paper [17], [18]. In this proposed work, three intensity features (mean, variance, standard deviation) and two texture features (Entropy, Energy) are calculated.

The rest of the paper is organized as follows. In section 2, the features extracted from MRI brain image by various feature extraction methods are reviewed. In section 3, the proposed feature extraction method from segmented MRI brain tissue images is discussed. Section 4 discusses the results and their analysis. In this section, the results are also compared with the conventional method. In the last section 5, conclusion is presented.

II. REVIEW OF PREVIOUS WORK ON MRI BRAIN IMAGE FEATURE EXTRACTION

Various MRI brain image feature extraction methods are listed in this section. The next step in the automated brain image segmentation and classification method is feature extraction. Feature extraction is the technique of extracting specific features from the pre-processed images. Various feature extraction methods have been cited in the literature for improving feature extraction process from MRI brain image.

Arivazhagan and Ganesan [19] used 2D wavelet transform based textural features for classification. In their work, initially basic statistical features are used and then co-occurrence based

textural features are used to improve the accuracy. An improved version based on wavelet packet decomposition is implemented by [21]. Their results revealed that the packet decomposition technique is more efficient than the 2D wavelet transform.

Ryszard [20] extracted features from local region apart from extracting the features from the whole image, which is used for image segmentation. Kekre and Tanuja [22] revealed that the entropy is the most dependable feature among the textural features.

Kadam et. al. [23] have used eight textural features: angular second moment, contrast, inverse difference moment, sum variance, sum entropy, entropy, and difference entropy and information measure of correlation to train the MLP network in segmenting brain tumor. Although the proposed method improves segmentation results, the qualitative and quantitative results given are inadequate.

Guler et. al. [27] presented an image segmentation system to automatically segment and label brain MR images to show normal and abnormal brain tissues using self-organizing maps (SOM) and knowledge-based expert systems. The feature vector is used as an input to the SOM. SOM is used to over segment images and a knowledge-based expert system is used to join and label the segments. Spatial distributions of segments extracted from the SOM are also considered as well as gray level properties. Segments are labeled as background, skull, white matter, gray matter, cerebrospinal fluid (CSF) and suspicious regions.

In [24], a fuzzy kohonen neural network is implemented for brain MR image segmentation. The technique used features like area, entropy, mean and standard deviation to segment tumor from brain MR image but did not use any preprocessing, for instance, noise removal to improve the extraction of these features. In addition, the qualitative and quantitative analyses of the proposed method are inadequate.

Joshi jayashri and phadke [26] proposed a method for segmenting tumour based on statistical structure analysis. The structural analysis was done for both tumour and normal tissues. The texture features have been extracted using co-occurrence matrix. Fuzzy c-means and an artificial neural network are used for classification. They proposed this method to examine the differences of texture features between macroscopic lesion white matter (LWM) and normal appearing white matter (NAWM) in magnetic resonance images with tumour and normal white matter (NWM)

Nandita ibraheem jabbar [25] proposed a technique for segmenting tumour, edema, white matter, gray matter and cerebrospinal fluid from FLAIR MRI brain images. In addition to tumour, they segmented edema as a separate class. In their technique, MRI brain images are segmented into 5 classes using k-means algorithm and calculated texture properties and features of wavelet energy function. They extracted the feature vectors from all the 5 segmented images by dividing the image into small blocks of size 4x4 pixels. The block feature vectors of all the segmented images are given as input to an artificial neural network using back propagation algorithm for classification.

III. PROPOSED BLOCK BASED FEATURE EXTRACTION FROM SEGMENTED IMAGES

The block diagram of the proposed method for feature extraction is shown in figure 1. In the proposed method, the segmented normal brain tissues such as gray matter, white matter, cerebrospinal fluid and pathological tissues (tumor) from our previous work [17], [18] are divided into 'N' number of blocks which is represented as B = {bn}; n = 1, 2, 3, ... N, as shown in figure 2. We have 128 blocks of size 4 x 4 as shown in figure 3, because the size of input MRI brain image is 512 x 512 pixels.

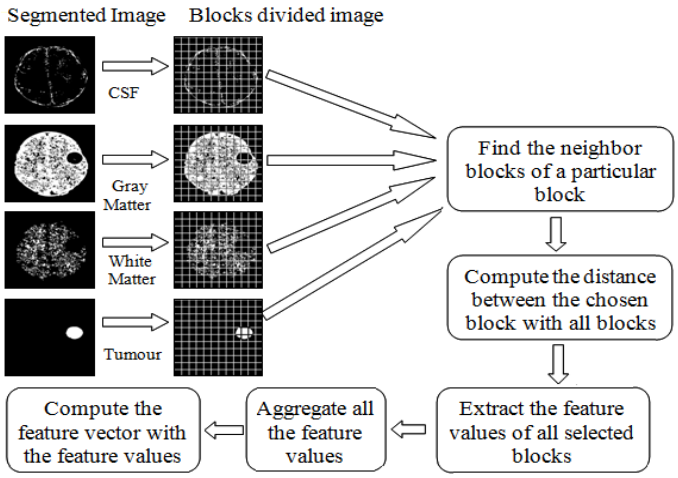

Fig. 1. Block diagram of proposed Feature Extraction Method

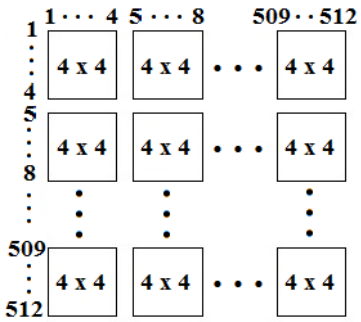

Fig. 2. Segmented image (512 x 512) broken down in to smaller blocks of size 4x4

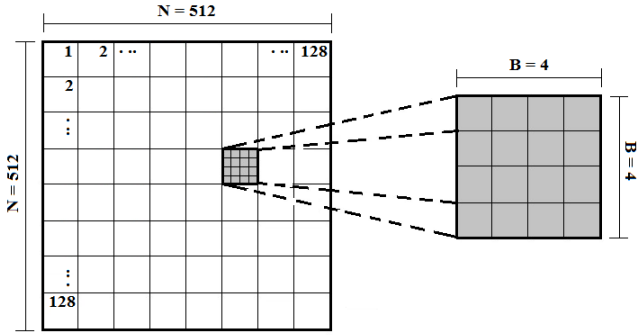

Fig. 3. Segmented Image (512 x 512) broken down in to 128 smaller blocks of size 4x4

For feature extraction process, we have taken a block b_n and checked this block with the neighbour blocks. If the entire neighbour block value is zero then these blocks are not considered for feature extraction process or else the distance between the chosen block and the neighbour block is determined by exploiting euclidian distance. $D_{nl} = b_n - b_l$; l = 1, 2, 3, ... N ($n \neq l$)

The distance value of each block D_{nl} is compared with the threshold value 't_1'. During the comparison, if the distance value D_{nl} of all blocks is less than the defined threshold value t_1, then it is adequate to store one block instead of storing all the blocks or else store the block's values individually. The obtained block values are stored in a variable $B_s = \{n'\}$; n′ = 1, 2, . . . N′ and the feature extraction process is carried out only for these stored blocks 'B_s'. The initial steps are as follows:

- Find the neighbor blocks of the entire divided blocks.
- Find the distance between all the neighbor blocks.
- Compare the distance value of each block with threshold value.
- Store all the blocks whose distance value is less than threshold value in a separate variable.
- Find the feature values of all the blocks stored in a variable.
- Find the average value of all the computed blocks' distance.
- Store all the features in a vector and fed as an input to the classifier.

Features can be extracted from the matrix to reduce feature space dimensionality and the formal definitions of chosen features from the matrix are done. The statistic feature's formula is depicted as below from equations (1) to (7).

A. Mean

The mean is defined as the sum of the pixel values divided by the total number of pixels values.

$$\text{Mean, } \mu = \frac{1}{mn}\sum_{i=1}^{m}\sum_{j=1}^{n} p(i,j) \qquad (1)$$

B. Variance

The variance is a parameter describing in part either the actual probability distribution of an observed population of numbers, or the theoretical probability distribution of a not-fully-observed population of numbers.

$$\text{Variance, } \sigma^2 = \frac{1}{mn}\sum_{i=1}^{m}\sum_{j=1}^{n}\left(p(i,j) - M\right)^2 \qquad (2)$$

C. Entropy

Entropy is a statistical measure of randomness that can be used to characterize the texture of the input image. Entropy is defined as,

$$\text{Entropy, } E_n = -\sum_{i=1}^{m}\sum_{j=1}^{n} p(i,j).\log p(i,j) \qquad (3)$$

D. Wavelet based Energy function

The feature vectors of the three energy functions of high frequency horizontal, vertical and diagonal sub-bands of the wavelet transform are extracted, since it reflects the texture properties.

$$\text{Energy, } E_{(H,V,D)} = \sum_{i=1}^{m}\sum_{j=1}^{n} p(i,j)^2 \qquad (4)$$

In order to obtain the three wavelet energies, the Haar wavelet transform is applied to each blocks of brain MRI image. Like all wavelet transforms, the Haar transform decomposes a discrete signal into two subsignals of half its length. One subsignal is a running average or trend and the other subsignal is a running difference or fluctuation.

The first trend subsignal, $a^1 = (a_1, a_2, \ldots\ldots a_{N/2})$ for the signal 'f' is computed by taking a running average in the following way. Its first value, 'a_1' is computed by taking the average of the first pair of values of f: $(f_1 + f_2)/2$ and then multiplying it by $\sqrt{2}$. i.e., $a1 = (f_1 + f_2)/\sqrt{2}$, continuing in this way all of the values of a^1 are produced by taking averages of successive pairs of values of 'f' and then multiplying these averages by $\sqrt{2}$. A precise formula for the values of a^1 is,

$$a_m = \frac{f_{2m-1} + f_{2m}}{\sqrt{2}}; \text{for} \quad m = 1, 2, 3, \ldots\ldots \frac{N}{2} \qquad (5)$$

The first fluctuation of the image f, which is denoted by $d^1 = (d_1, d_2, \ldots\ldots d_{N/2})$ is computed by taking a running difference in the following way. Its first value, 'd_1' is computed by taking the half the difference of the first pair of values of f: $(f_1 - f_2)/2$ and then multiplying it by $\sqrt{2}$. i.e., $d1 = (f_1 - f_2)/\sqrt{2}$, continuing in this way all of the values of d^1 are produced by taking running difference of successive pairs of values of 'f' and then multiplying these averages by $\sqrt{2}$. A precise formula for the values of d^1 is,

$$d_m = \frac{f_{2m-1} - f_{2m}}{\sqrt{2}}; \text{for} \quad m = 1, 2, 3, \ldots\ldots \frac{N}{2} \qquad (6)$$

The following denotation is used; 'A' is the approximation area that includes information of the average of the image, 'H' is the horizontal area that includes information about the vertical details in the image, 'V' is the vertical area that includes information about the horizontal details in the image and 'D' is the diagonal area that includes information about the diagonal details.

After Haar transform, the approximation component contains most of the energy and the diagonal component contains less energy. Thus 1-level Haar transform has kept the energy constant. After a one level wavelet transform, a 4×4 pixel block is decomposed into four frequency bands of 2×2 coefficients as shown in figure 4. For example, the coefficients in horizontal band of one block are H_1, H_2, H_3, H_4, in vertical band V_1, V_2, V_3, V_4 and in diagonal band D_1, D_2, D_3 and D_4. Then horizontal energy E_H, vertical energy E_V and diagonal energy E_D are combined to attain the feature value of the energy. The training feature vector 'Fv' is defined by Equation (7) by combining all the extracted features like mean M, variance σ2, entropy E and the energy E (H, V, D).

$$Fv = [f(M), f(\sigma^2), f(E), f(E_H), f(E_V), f(E_D)] \qquad (7)$$

A_1	A_2	H_1	H_2
A_3	A_4	H_3	H_4
V_1	V_2	D_1	D_2
V_3	V_4	D_3	D_4

Fig. 4. 4×4 pixel block is decomposed into four frequency bands of 2×2 coefficients

IV. Experimental results and discussion

This section illustrates the experimental results of our proposed feature extraction technique using brain MRI images with and without tumors. Our proposed approach is implemented in Matlab environment on Core i5, 1.8 GHZ processor installed with MATLAB 7.13.

The MRI image dataset that we have utilized in our proposed technique is taken from diagnostic centers and publicly available sources. This image dataset contains 50 brain MRI images with and without tumor. Fig. 5 and Fig. 6 shows the input MRI brain image datasets of normal and abnormal images. The Fig. 7 and Fig 8. shows the segmented tissues of some of the sample MRI normal and abnormal brain images and Tables I to IV shows the extracted feature values of segmented tissues of sample normal and abnormal MRI brain images.

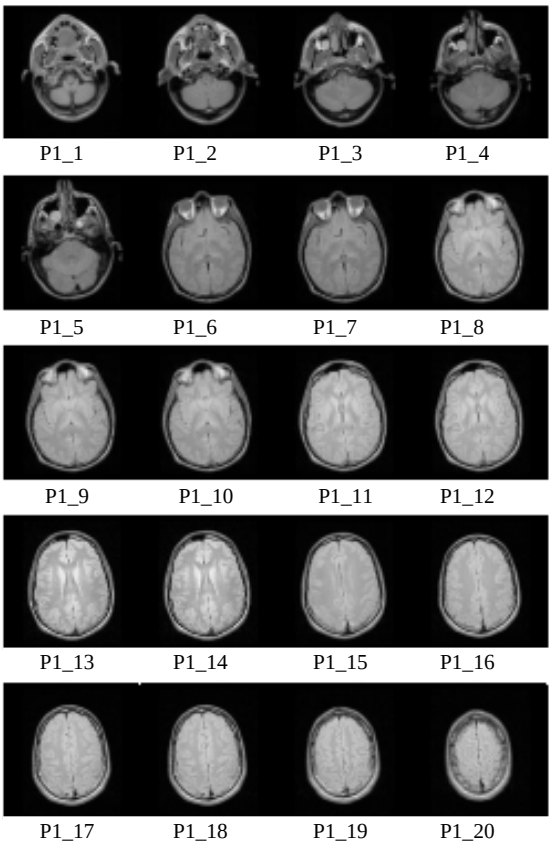

Fig. 5 Dataset of patient 1 without tumour

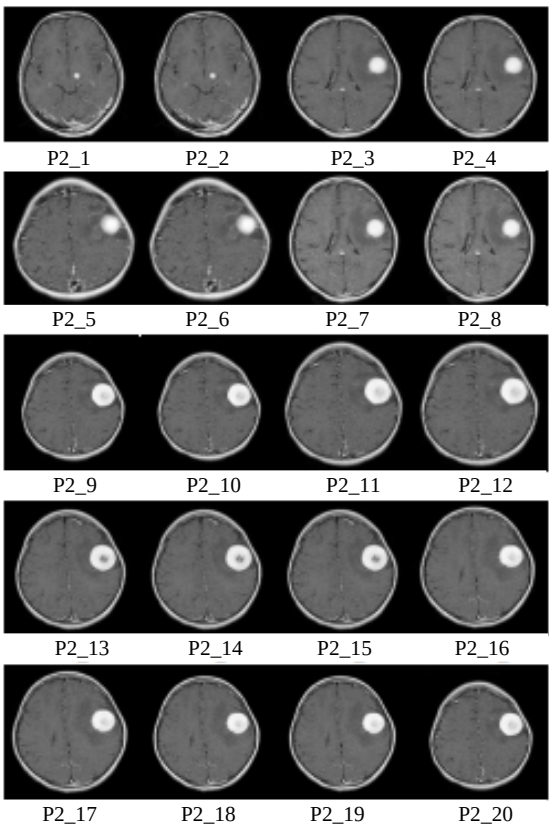

Fig. 6 Dataset of patient 2 with benign tumour

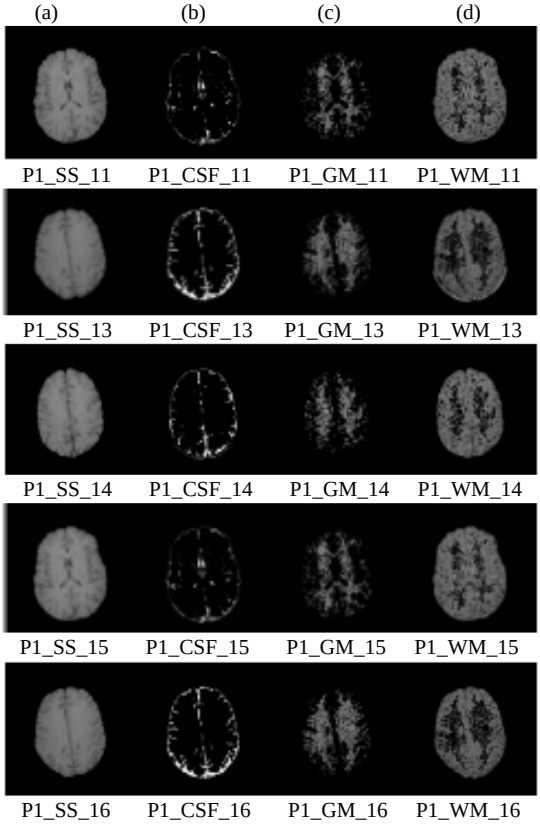

Fig. 7. Segmented brain tissues of patient 1 dataset: Column a) skull stripped b) CSF c) GM d) WM

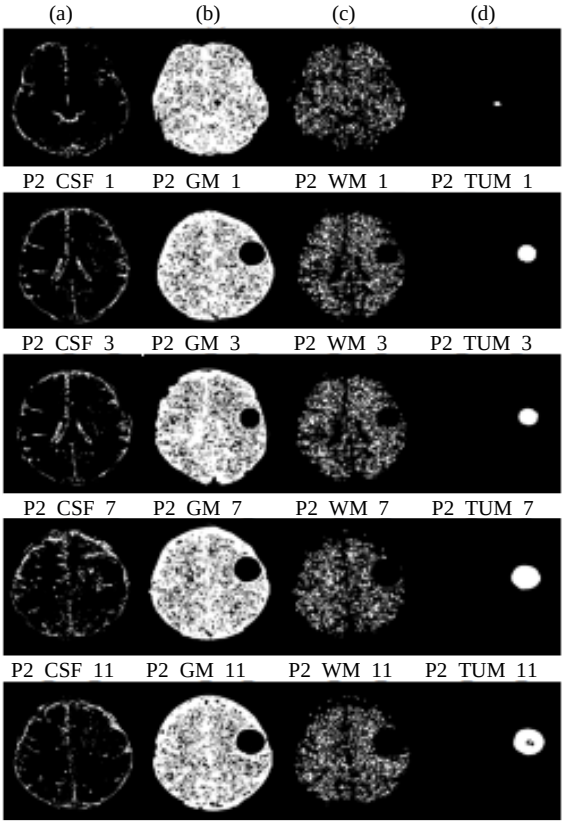

Fig. 8 Segmented brain tissues of patient 2 dataset: Column a) CSF b) GM c) WM d) Tumour

TABLE I. TABLE 1. MEAN VALUE OF NORMAL AND ABNORMAL BRAIN MR IMAGES

Image	CSF	WM	GM	Tumour
P1_1	0.345	44.872	72.304	171.276
P1_2	0.375	37.968	65.935	172.505
P1_3	0.306	36.251	66.513	183.022
P1_4	0.310	39.136	72.210	176.718
P1_5	0.351	36.685	72.679	184.939
P1_6	0.475	40.540	67.164	170.558
P1_7	0.336	41.627	72.687	184.576
P1_8	0.473	37.747	68.092	175.466
P1_9	0.456	44.189	65.247	176.900
P1_10	0.324	38.478	68.760	161.752
P2_1	0.678	22.534	44.997	16.211
P2_2	0.668	21.929	54.508	18.337
P2_3	0.665	17.165	56.900	17.978
P2_4	0.813	18.108	55.852	10.384
P2_5	0.655	15.577	46.737	19.670
P2_6	0.882	19.309	40.534	13.250
P2_7	0.729	28.843	54.711	12.036
P2_8	0.584	23.590	48.591	13.128
P2_9	0.642	15.960	57.498	13.228
P2_10	0.571	23.146	41.194	13.037

TABLE II. TABLE 2 VARIANCE VALUE OF NORMAL AND ABNORMAL BRAIN MR IMAGES

Image	CSF	WM	GM	Tumour
P1_1	0.425	1330.910	871.183	955.876
P1_2	0.450	1342.535	869.248	927.369
P1_3	0.375	1318.418	896.695	851.290
P1_4	0.425	1354.268	831.405	847.751
P1_5	0.372	1346.192	820.417	913.412
P1_6	0.337	1317.677	887.420	830.854
P1_7	0.398	1353.680	862.746	843.178
P1_8	0.414	1330.580	898.384	992.117
P1_9	0.368	1313.191	844.678	1025.400
P1_10	0.395	1353.455	889.323	932.445
P2_1	0.144	946.029	402.884	3188.861
P2_2	0.134	880.291	383.467	3189.518
P2_3	0.134	767.345	385.076	2491.400
P2_4	0.147	904.869	400.464	2756.097
P2_5	0.147	793.974	414.391	3437.424
P2_6	0.148	1030.116	399.639	2315.579
P2_7	0.126	914.606	429.825	2354.539
P2_8	0.140	978.626	412.542	3333.341
P2_9	0.134	1011.786	384.663	2218.553
P2_10	0.143	836.841	407.521	3519.861

TABLE III. TABLE3. ENTROPY VALUE OF NORMAL AND ABNORMAL BRAIN MR IMAGES

Image	CSF	WM	GM	Tumour
P1_1	0.689	0.737	0.432	0.425
P1_2	0.698	0.735	0.427	0.384
P1_3	0.707	0.734	0.404	0.387
P1_4	0.729	0.732	0.441	0.373
P1_5	0.725	0.740	0.420	0.278
P1_6	0.726	0.736	0.424	0.408
P1_7	0.693	0.739	0.417	0.339
P1_8	0.713	0.733	0.469	0.515
P1_9	0.718	0.737	0.424	0.383
P1_10	0.724	0.739	0.404	0.376
P2_1	0.638	0.730	0.317	0.627
P2_2	0.631	0.724	0.282	0.705
P2_3	0.634	0.730	0.275	0.623
P2_4	0.625	0.728	0.305	0.669
P2_5	0.670	0.727	0.298	0.704
P2_6	0.629	0.724	0.314	0.685
P2_7	0.662	0.725	0.352	0.682
P2_8	0.641	0.730	0.308	0.668
P2_9	0.630	0.730	0.264	0.629
P2_10	0.632	0.721	0.308	0.678

TABLE IV. TABLE4. HORIZONTAL ENERGY VALUE OF NORMAL AND ABNORMAL BRAIN MR IMAGES

Image	CSF	WM	GM	Tumour
P1_1	1.592	16.389	13.426	12.462
P1_2	1.560	16.352	13.314	12.467
P1_3	1.658	15.783	13.442	12.288
P1_4	1.677	16.403	12.900	12.474
P1_5	1.551	16.471	13.613	12.575
P1_6	1.619	16.411	12.684	12.296
P1_7	1.649	15.772	13.056	12.674
P1_8	1.659	16.173	12.650	12.426
P1_9	1.676	16.181	13.154	12.085
P1_10	1.619	15.938	13.882	12.370
P2_1	1.392	13.872	10.768	21.666
P2_2	1.471	14.433	10.275	21.753
P2_3	1.439	13.677	10.384	21.748
P2_4	1.496	13.954	10.721	23.053
P2_5	1.468	14.619	10.594	21.224
P2_6	1.458	14.226	10.479	21.397
P2_7	1.451	14.181	10.355	22.844
P2_8	1.410	14.158	10.446	23.018
P2_9	1.464	14.002	10.674	22.316
P2_10	1.402	13.628	10.623	23.195

TABLE V. TABLE5 VERTICAL ENERGY VALUE OF NORMAL AND ABNORMAL BRAIN MR IMAGES

Image	CSF	WM	GM	Tumour
P1_1	1.544	15.526	12.040	12.836
P1_2	1.560	15.560	12.017	12.408
P1_3	1.547	15.449	12.143	11.635
P1_4	1.532	15.499	12.184	12.904
P1_5	1.605	15.269	12.275	12.779
P1_6	1.543	15.377	12.390	12.307
P1_7	1.542	15.493	12.441	12.879
P1_8	1.540	15.286	12.439	13.917
P1_9	1.602	15.317	12.109	13.951
P1_10	1.547	15.392	12.482	13.465
P2_1	1.500	14.569	10.573	21.316
P2_2	1.437	14.898	10.519	18.811
P2_3	1.483	14.178	11.020	20.658
P2_4	1.475	14.662	10.946	21.448
P2_5	1.506	14.853	10.566	18.992
P2_6	1.498	14.517	11.083	17.633
P2_7	1.501	14.439	11.167	18.253
P2_8	1.473	14.432	10.648	19.670
P2_9	1.449	14.161	10.733	16.636
P2_10	1.472	14.383	10.681	18.378

TABLE VI. TABLE6 DIAGONAL ENERGY VALUE OF NORMAL AND ABNORMAL BRAIN MR IMAGES

Image	CSF	WM	GM	Tumour
P1_1	1.288	12.970	9.844	12.125
P1_2	1.320	13.022	9.860	7.493
P1_3	1.312	12.927	9.901	8.227
P1_4	1.247	13.036	10.024	7.931
P1_5	1.339	13.025	9.651	12.478
P1_6	1.325	12.992	9.940	8.062
P1_7	1.331	13.042	9.946	8.521
P1_8	1.335	12.911	9.886	9.819
P1_9	1.238	13.047	9.789	10.733
P1_10	1.225	13.014	9.640	12.171
P2_1	1.170	12.237	7.649	18.962
P2_2	1.173	12.654	8.472	18.220
P2_3	1.182	12.462	9.178	14.683
P2_4	1.173	12.214	7.939	17.393
P2_5	1.187	12.492	9.142	18.558
P2_6	1.183	11.980	8.066	14.681
P2_7	1.185	12.678	9.011	14.972
P2_8	1.172	12.394	9.016	15.889
P2_9	1.181	12.189	8.604	14.528
P2_10	1.190	12.329	8.448	15.565

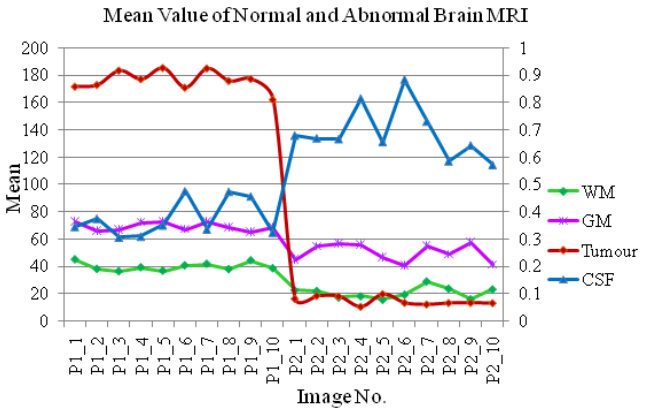

Fig. 9. Mean values of normal and abnormal brain MR images

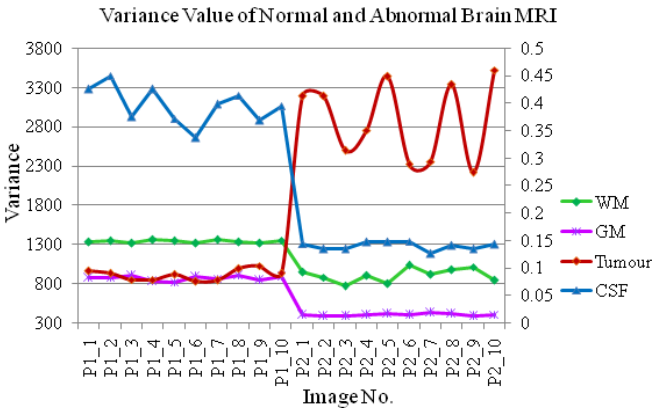

Fig. 10. Variance values of normal and abnormal brain MR images

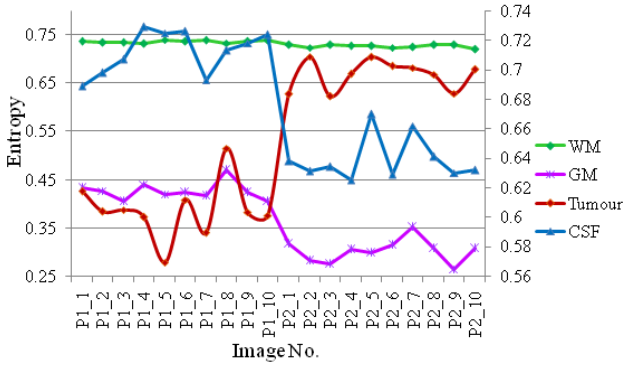

Fig. 11. Entropy values of normal and abnormal brain MR images

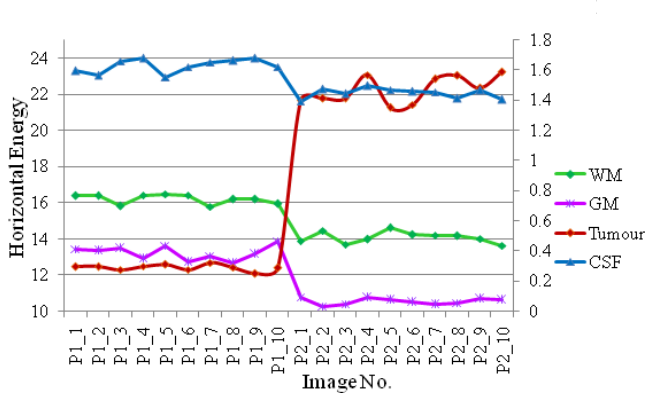

Fig. 12. Horizontal energy values of normal and abnormal brain MR images

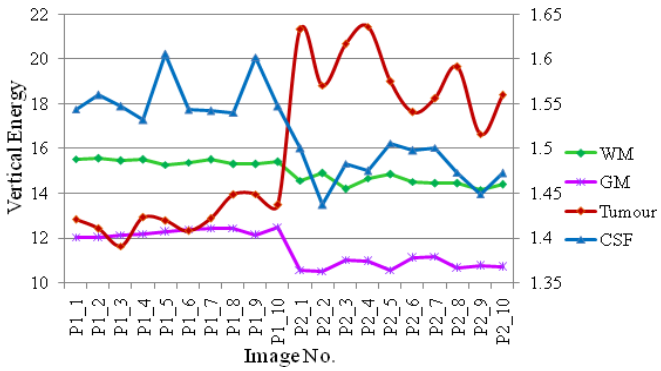

Fig. 13. Vertical energy values of normal and abnormal brain MR images

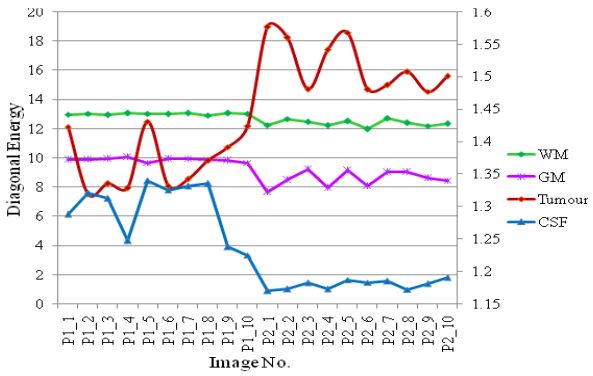

Fig. 14. Diagonal energy values of normal and abnormal brain MR images

V. CONCLUSION

In this paper, the features values are extracted based on block extraction method instead of extracting the features values for the entire image. so, the computation time can be reduced by calculating the feature values only for the selective blocks. Next in this paper instead of calculating all feature values, only selective feature values which is enough to give promising result is calculated. Intensity based features like mean, variance and texture based features like entropy and energy is calculated. Haar wavelet transform is used to obtain the horizontal, vertical and diagonal energy.

From the graphs (Figures 9 to 14), it was found that the feature values (mean, variance, entropy, horizontal energy, vertical energy, and diagonal energy) for normal and abnormal images could be easily distinguished. It was also found that all the calculated feature values (except mean) of the tumour were higher compared with the other tissues. At last, the calculated feature values can be combined as a vector to feed as input to a classifier to detect brain diseases like Schizophrenia and Alzheimer disease.

REFERENCES

[1] P. Lin, Y. Yang, C. X. Zheng and J.W Gu, “An Efficient Automatic Framework for Segmentation of MRI Brain Image,” *Proceedings of the Fourth International Conference on Computer and Information Technology (CIT’04), IEEE.*, 2004.

[2] A. P. Zijdenbos, B. M. Dawant, “Brain segmentation and white matter lesion detection in MR images,” *Critical Reviews in Biomedical Engineering*, Vol. 22, 1994, pp. 401–465.

[3] Hajer Jlassi, Kamel Hamrouni, "Interactive Three-Dimensional Segmentation of MR Images by Hierarchical Watershed", *IRECOS*, Vol. 4, no. 2, pp. 183 - 187, March 2009.

[4] J. Chiverton, K. Wells, E. Lewis, C. Chen, B. Podda, D. Johnson, “Statistical morphological skull stripping of adult and infant MRI data,” *Computers in Biology and Medicine*, Vol. 37, No.3, 2007, pp. 342-357.

[5] B. Dogdas, D.W. Shattuck, R.M Leahy, “Segmentation of skull and scalp in 3-D human MRI using mathematical morphology,” *Human Brain Mapping*, Vol. 26, No. 4, 2005, pp. 273 - 285.

[6] C.A. Cocosco, A. P. Zijdenbos, A. C. Evans, “A fully automatic and robust brain MRI tissue classification method” *Med. Image Anal.* Vol. 7, 2003, pp. 513–527.

[7] C. S. Drapaca, V. Cardenas, C. Studholme, “Segmentation of tissue boundary evolution from brain MR image sequences using multi-phase level sets,” *Computer Vision and Image Understanding*, Vol. 100, 2005, pp. 312 - 329, No. 3.

[8] K. A. Ganser, H. Dickhaus, R. Metzner, C. R. Wirtz, “A deformable digital brain atlas system according to Talaicrach and Tournoux,” *Medical Image Analysis*, vol. 8, no. 1, 2004, pp. 3–22.

[9] Güler, İ., Demirhan, A. and Karakıs, R. “Interpretation of MR images using self-organizing maps and knowledge-based expert systems,” *Digital Signal Processing*, Vol. 19 , No. 4, 2009, pp. 668-677.

[10] C. Heil, D. Walnut, “Continuous and discrete wavelet transforms,” *SIAM Rev*., Vol. 31, 1989, pp. 628–666.

[11] P. Hore, L. O. Hall, D. B. Goldgof, Y. Gu, A. A. Maudsley, "A Scalable Framework For Segmenting Magnetic Resonance Images," *Journal of Signal Processing Systems*, Vol. 54 , No. 1-3, 2009, pp. 183 - 203.

[12] N. I Jabbar, M. Mehrotra, "Application of Fuzzy Neural Network for Image Tumor Description," *Proceedings of World Academy of Science, Engineering and Technology*, Vol: 34, 2008.

[13] J. Kong, J. Wang, Y. Lu, J. Zhang, Y. Li, and B. Zhang, "A novel approach for segmentation of MRI brain images," *IEEE Mediterranean Electrotechnical Conference*," MELECON, pp. 525 – 528, 2006.

[14] W. Kuo, C. Lin, Y. Sun, "Brain MR images segmentation using statistical ratio: Mapping between watershed and competitive Hopfield clustering network algorithms," *Computer Methods and Programs in Biomedicine*, Vol. 91, No. 3, 2008, pp. 191-198.

[15] H. A. Legal-Ayala, J. Facon, "Automatic segmentation of brain MRI through learning by example," *proceedings of International Conference on Image Processing*, (ICIP '04.), Vol. 2, pp. 917- 920, 2004.

[16] Y. Li, Z. Chi, "MR Brain Image Segmentation Based on Self-Organizing Map Network," *International Journal of Information Technology*, Vol. 11, No. 8, 2005.

[17] D. Selvaraj, R. Dhanasekaran, "Segmentation of cerebrospinal fluid and internal brain nuclei in brain magnetic resonance images," *IRECOS*, Vol.8, issue 5, 2013, pp.1063-1071.

[18] D. Selvaraj, R. Dhanasekaran, "Combining Tissue Segmentation and Neural Network for Brain tumour Detection", *IAJIT*, Vol.12. No.1.

[19] S. Arivazhagan, L. Ganesan, "Texture classification using wavelet transforms," *Pattern Recognition Letters*, 2003; 24:1513-21.

[20] S. Ryszard, "Image feature extraction techniques and their applications for CBIR and biometrics system," *International Journal of Biology and Biomedical Engineering*, 2007;1:6-16.

[21] P. Hiremath, S. Shivashankar, "Texture classification using wavelet packet decomposition," *Graphics, Vision and Image Processing Journal*, 2006; 6:77-80.

[22] H. Kekre, S. Tanuja, G. Saylee, "Detection and demarcation of tumor using vector quantization in MR images," *International Journal of Engineering Science and Technology*, 2009; 1:59-66.

[23] D. B. Kadam, S. S. Gade, M. D. Uplaneand, R. K. Prasad, "Neural Network Based Brain Tumor Detection Using MR Images," *International Journal of Computer Science and Communication (IJCSC)*, Vol. 2, No.2, July -Dec. 2011, pp. 325-331.

[24] Nahla Ibraheem Jabbar and Monica Mehrotra, "Application of Fuzzy Neural Network for Image Tumor Description," *World Academy of Science, Engineering and Technology*, Issue. 20, August 2008, pp. 575-577.

[25] Nandita pradhan and sinha, "Development of a composite feature vector for the detection of pathological and healthy tissues in FLAIR MR images of brain," *Journal of ICGST-BIME*, Vol.10, No.1, pp. 1 – 11, Dec 2010.

[26] Joshi Jayashri, phadke, "Feature extraction and texture classification in MRI," *In proceedings of international conference on computer technology*, Vol. 2, pp. 130 – 136, 2010.

[27] L. Guler, A. Demirhan, R. Karakıs, "Interpretation of MR images using self-organizing maps and knowledge-based expert systems," *Digital Signal Processing*, Vol. 19 , No. 4, 2009, pp. 668-677.